NASA Technical Memorandum 100831

A Viscoplastic Theory Applied to Copper

(NASA-TM-100831) A VISCOPLASTIC THEORY APPLIED TO COPPER (NASA) 15 p CSCL 20K

N88-21497

Unclas
G3/39 0136188

Alan D. Freed and Michael J. Verrilli
Lewis Research Center
Cleveland, Ohio

Prepared for the
International Seminar on "The Inelastic Behaviour of Solids: Models and Utilization"
sponsored by MECAMAT
Besançon, France, August 30–September 1, 1988

NASA

A VISCOPLASTIC THEORY APPLIED TO COPPER

Alan D. Freed and Michael J. Verrilli
National Aeronautics and Space Administration
Lewis Research Center
Cleveland, Ohio 44135

E-4020

SUMMARY

A phenomenologically based viscoplastic model is derived for copper. The model is thermodynamically constrained by the condition of material dissipativity. Two internal state variables are considered. The back stress accounts for strain-induced anisotropy, or kinematic hardening. The drag stress accounts for isotropic hardening. Static and dynamic recovery terms are not coupled in either evolutionary equation. The evolution of drag stress depends on static recovery, while the evolution of back stress depends on dynamic recovery. The material constants are determined from isothermal data. Model predictions are compared with experimental data for thermomechanical test conditions. They are in good agreement at the hot end of the loading cycle, but the model over predicts the stress response at the cold end of the cycle.

INTRODUCTION

A wide range of materials are used in devices that are designed to function in high-temperature environments. Materials of high-temperature capability limit the designer in some applications, while materials of high-conductivity capability limit him in other applications. Whenever a design application calls for a material of high conductivity, copper is often the material of choice. For example, a copper liner is used in the regeneratively-cooled main combustion chamber of the space shuttle main engines.

The prime objective in the development of a viscoplastic model, in the authors' opinion, is to make it as simple as the physics and intended application allows. The main reason for doing inelastic analyses is not to determine the deformation response of a structure per se, but rather, to assess its useful service life. Results from inelastic analyses are input to life assessing schemes. These schemes typically require such quantities as: stress range, mean stress, inelastic strain range, and percentages of creep and plasticity that make up the inelastic strain range. It is therefore paramount that the predictive capability of a viscoplastic model be capable of predicting these phenomena with reasonable accuracy.

A viscoplastic model for pure metals is developed and applied to copper in this paper. (Its extension to alloys is a subject of current research.) This model is phenomenological, and consistent with the physics of inelastic deformation in pure metals. Its mathematical structure is kept simple but adequate, so that the model may be useful. Material constants are determined in a straight forward manner from isothermal data. To begin to assess the model's predictive capability, predictions are compared with experiments for the case of thermomechanical deformation.

NOMENCLATURE

A,Do,Ds,h,H,L,n,Q,S,Tm	inelastic material constants
B_{ij}	back stress (deviatoric)
D	drag stress
E,α,ν	elastic material constants
$e_{ij} = \varepsilon_{ij} - 1/3\ \varepsilon_{kk}\delta_{ij}$	deviatoric strain
$\underline{F},\underline{g},\underline{G},\underline{r},\underline{R},\underline{Z},\Theta$	inelastic material parameters
k,T,ΔT	Boltzmann's constant, absolute temperature, temperature change
$S_{ij} = \sigma_{ij} - 1/3\ \sigma_{kk}\delta_{ij}$	deviatoric stress
$X_2 = \sqrt{\frac{1}{2} X_{ij}X_{ji}}$	norms $X_2 = \left\{S_2, B_2, \Sigma_2, \varepsilon_2^p, \varepsilon_2^c\right\}$
δ_{ij}	Kronecker delta
ε_{ij}	strain
ε_{ij}^p, ε_{ij}^c	inelastic strains (deviatoric)
σ_{ij}	stress
$\Sigma_{ij} = S_{ij} - B_{ij}$	effective stress (deviatoric)

VISCOPLASTIC THEORY

The viscoplastic theory presented herein incorporates two internal state variables; they are: the back stress B_{ij} for kinematic or flow-induced anisotropic hardening (which is deviatoric), and the drag stress D for isotropic hardening. A simplified structure for this theory is assumed so that there is no coupling between static and dynamic recovery terms in either of the evolutionary equations. This facilitates the derivation of material functions for the viscoplastic model presented later in the paper.

The proposed elastic-viscoplastic theory is characterized by the elastic constitutive equations

$$\sigma_{kk} = \frac{E}{1 - 2\nu}\left(\varepsilon_{kk} - 3\alpha\,\Delta T\right) \tag{1a}$$

and

$$S_{ij} = \frac{E}{1 + \nu}\left(e_{ij} - \varepsilon_{ij}^p\right) \tag{1b}$$

and by the viscoplastic constitutive equations (cf. Freed (ref. 1))

$$\dot{\varepsilon}^p_{ij} = \Theta \, \underline{Z}(\underline{F}) \, \frac{\Sigma_{ij}}{\Sigma_2} \tag{2a}$$

$$\dot{B}_{ij} = H\left(\dot{\varepsilon}^p_{ij} - \frac{B_{ij}}{L} \, \dot{\varepsilon}^p_2\right) \tag{2b}$$

and

$$\dot{D} = h\left(\frac{\dot{\varepsilon}^p_2}{\underline{G}} - \Theta \, \underline{r}(\underline{G})\right) \tag{2c}$$

where

$$\underline{F} = \frac{\Sigma_2}{D} \quad \text{and} \quad \underline{G} = \underline{g}(D) \tag{3}$$

Repeated indicies are summed over. A dot placed over a variable denotes its time rate of change. Strains, displacements, and rotations of the material element are infinitesimal.

The flow equation, equation (2a), is consistent with the constructs used by Prager (ref. 2) in his theory of plasticity. Contracting this equation with itself results in the relationship

$$\underline{Z}(\underline{F}) = \frac{\dot{\varepsilon}^p_2}{\Theta} \tag{4}$$

which defines the Zener-Hollomon (ref. 3) parameter.

The evolutionary equation for back stress, equation (2b), is consistent with the kinematic constructs used by Krieg (ref. 4) in his two-surface theory of plasticity. Here strain-induced dynamic recovery competes against strain hardening. This competitive process results in the back stress hardening up exponentially to a limiting state L associated with kinematic saturation, and thereby accounting for the strain hardening response observed in stable hysteresis loops of stress versus strain.

The evolutionary equation for drag stress, equation (2c), is consistent with the isotropic constructs used by Mitra and McLean (ref. 5) in their theory of creep. Here thermally-induced static recovery competes against strain hardening. This competitive process accounts for the cyclic strain hardening response observed early in the fatigue life.

For any viscoplastic theory to be thermodynamically admissible, it must satisfy dissipativity (cf. Onat and Leckie (ref. 6)). For the viscoplastic theory of equation (2), this condition requires that (ref. 1)

$$\sigma_{ij}\dot{\varepsilon}^p_{ji} \geq B_{ij} \, \frac{\dot{B}_{ij}}{H} + D \, \frac{\dot{D}}{h} \tag{5a}$$

resulting in the constraint

$$\underline{r} \geq \underline{Z}\left[\frac{1}{\underline{G}} - 2\left(\underline{F} + \frac{B_2^2}{LD}\right)\right] \tag{5b}$$

which bounds static recovery from below. This constraint will seldom, if ever, be realized in any given analysis but, nevertheless, it is a physically mandatory constraint. Static recovery is bound from below by another constraint, too. The drag stress cannot dip below the minimum value D_o associated with the virgin or annealed state.

STEADY-STATE FLOW

Before the viscoplastic theory of the previous section can be used to model a material or a class of materials, specific forms for its material functions Θ, $\underline{r}$, and $\underline{Z}$ must be determined. Physically-based phenomenological relations are used to meet this need. In this section, conditions of steady-state flow are used to characterize the thermal diffusivity Θ and Zener-Hollomon $\underline{Z}$ parameters.

The temperature dependence of this theory is largely contained within the thermal diffusivity parameter which is taken to be (cf. Miller (ref. 7)).

$$\Theta = \begin{cases} \exp\left(\dfrac{-Q}{kT}\right) & ; \quad T \geq \dfrac{T_m}{2} \\ \exp\left\{\dfrac{-2Q}{kT_m}\left[\ell n\left(\dfrac{T_m}{2T}\right) + 1\right]\right\} & ; \quad T \leq \dfrac{T_m}{2} \end{cases} \tag{6}$$

Diffusion-controlled dislocation climb is the primary rate controlling mechanism of inelastic flow at the higher homologous temperatures, while dislocation glide dominates at the lower homologous temperatures (cf. Ashby (ref. 8)). Equation 6 represents the effect that these mechanisms have on the temperature dependence of inelastic flow in a simplistic way.

Since the steady-state flow of metals can be modeled by a power-law at the lower stresses and an exponential at the higher stresses (cf. Dorn (ref. 9)), one can write the steady-state Zener-Hollomon parameter as

$$\underline{Z}\left(\frac{S_2}{S}\right) = \begin{cases} A\left(\dfrac{S_2}{S}\right)^n & ; \quad S_2 \leq S \\ A \exp\left[n\left(\dfrac{S_2 - S}{S}\right)\right] & ; \quad S_2 \geq S \end{cases} \tag{7a}$$

which is associated with the flow equation

$$\dot{\varepsilon}^c_{ij} = \theta \underline{Z}\left(\frac{S_2}{S}\right) \frac{S_{ij}}{S_2} \tag{7b}$$

of Odqvist's (ref. 10) theory of creep. This Zener-Hollomon parameter is defined in such a way that it is continuous and differentiable across the interface $S_2 = S$. Diffusion-controlled dislocation climb governs the inelastic response at the lower stresses, while dislocation glide governs it at the higher stresses (ref. 8). Equation 7 represents the effect that these mechanisms have on the stress dependence of inelastic flow in a simplistic way.

VISCOPLASTIC MODEL

A specific viscoplastic model is formulated in this section by equating the arguments of the transient and steady-state Zener-Hollomon parameters of equations (2) and (7) under steady-state conditions. This enables one to derive specific representations for the Zener-Hollomon $\underline{Z}$ and static recovery $\underline{r}$ parameters that apply to transient and steady-state conditions alike.

Equating these arguments at steady state gives the equation

$$\underline{F} = \frac{\Sigma_2}{D} = \frac{S_2 - B_2}{D} = \frac{S_2 - L}{D} = \frac{S_2}{S} \tag{8a}$$

thereby enabling one to define the function

$$\underline{G} = \frac{L}{S - D} = \frac{S_2}{S} \tag{8b}$$

for static recovery at steady state, where $0 < D < S$. This derivation makes use of the facts that $\Sigma_2 = S_2 - B_2$ and $B_2 = L$ at steady state (neither of which is true, in general).

With the structure of the function $\underline{G}$ now established, it is useful to reconsider the evolutionary equation for the drag stress, equation (2c). Therein, the drag stress is defined to harden up at the rate $h\dot{\varepsilon}^p_2/G$, which equals $h(S - D)\dot{\varepsilon}^p_2/L$ because of equation (8). Therefore, like the back stress, the drag stress hardens up in an exponential manner. That is, this evolutionary equation for drag stress has the concept of dynamic recovery built in without introducing a separate term for it. However, unlike the back stress, the effect of strain hardening can never be completely canceled out by the influence of dynamic recovery at the isotropic saturation of state. The influence of static recovery is also required. This is because the drag stress D must always be less than the power-law breakdown stress S in the presence of a back stress B_{ij}.

By combining equations (7) and (8), one obtains the desired Zener-Hollomon parameter

$$\underline{Z}(\underline{F}) = \begin{cases} A\,\underline{F}^{n} & ; \quad \underline{F} \le 1 \\ A\,\exp[n(\underline{F}-1)] & ; \quad \underline{F} \ge 1 \end{cases} \tag{9a}$$

Likewise, by combining equations (8) and (9a), one obtains the desired static recovery parameter

$$\underline{r}(\underline{G}) = \begin{cases} 0 & ; \quad D = Do \\ \underline{R}(\underline{G}) & ; \quad D > Do \end{cases} \tag{9b}$$

where

$$\underline{R}(\underline{G}) = \begin{cases} A\,\underline{G}^{n-1} & ; \quad \underline{G} \le 1 \\ A\,\exp[n(\underline{G}-1)]/\underline{G} & ; \quad G \ge 1 \end{cases} \tag{9c}$$

since $\underline{r} = \underline{Z}/\underline{G}$ and $\underline{G} = \underline{F}$ at steady state. This static recovery parameter is thermodynamically constrained by equation (5).

Since $\underline{F}$ and $\underline{G}$ are not restricted to be steady-state parameters, the Zener-Hollomon and static-recovery parameters of equation (9) apply to transient and steady-state conditions alike.

DETERMINING MATERIAL CONSTANTS

For the viscoplastic model presented in this paper, there are two material constants required to characterize thermal diffusivity: Q and Tm; three material constants required to characterize steady state: A, n, and S; three material constants required to characterize transient behavior: h, H, and L; and one initial condition: Do. Thus, there are nine viscoplastic material constants in all. Their values for copper are given in table I. Of these nine, only four can vary with temperature; they are: h, H, L, and Do.

The activation energy for self diffusion Q and the melting temperature Tm are handbook data.

With the thermal diffusivity now characterized, one can determine the Zener-Hollomon parameter $\underline{Z} = \dot{\epsilon}_2^c/\Theta$ at steady state and plot it against its associated flow stress S_2. Such a data plot is presented in figure 1 for copper. Each datum point from the literature represents the average of typically four to six creep experiments, usually run at different temperatures but with the same flow stress. Our fully-reversed saturated cyclic data are in agreement with these monotonic data. Values for the material constants A, n, and S are obtained by fitting these data to equation (7a). Such a fit is represented by the solid curve in this figure for the material constants given in table I. These constants are quickly obtained by trial and error. The coefficient A translates the curve along the ordinate, the Norton exponent n defines the slope of the curve in the power-law domain, and the power-law breakdown stress S splits the stress domain into power-law and exponential stress-dependent domains.

With the thermal-diffusivity and steady-state material constants specified, one can determine the material constants H and L from stable, stress-strain, hysteresis loops, where the drag stress is saturated. Actually, an interactive, nonlinear, least-squares, optimization program (ref. 15) was used to fit H, L, and the saturated value of the drag stress Ds to data obtained from stabie hysteresis loops at room-temperature, 200, 400, and 600 °C. Although it is not necessary to use such a technique, it is useful and expedient to do so in determining these particular material constants. An optimization algorithm is also an extremely useful tool in assessing the validity of proposed constitutive equations. The optimized values for H and Ds were found to be independent of temperature, and their averaged values were determined. Only L varied systematically with temperature, and was fit with good accuracy by an Arrhenius function of temperature (see table I). The experimental and correlated, stable, stress-strain, hysteresis loops are presented in figure 2 for your comparison. The material constant L determines the extent of increase in stress from the onset of inelastic flow to the saturated state. The material constant H determines how much inelastic strain is required to go from the onset of inelastic flow to the saturated state. The fact that the limiting state of back stress L diminishes with increasing temperature introduces the effect of static recovery without introducing a separate term for it into the evolutionary equation for back stress.

Two material constants remain to be determined; they are: Do and h. Their values are quickly obtained by trial and error by comparing numerical simulations with experiments. The virgin drag stress Do is associated with the annealed yield strength. The material constant h determines the rate of isotropic hardening, and can be determined from the first few stress-strain cycles from the same experiments used to quantify the constants H and L at isotropic saturation. The experimental and correlated stress-strain hysteresis loops at 200 °C are presented in figure 3 for your comparison.

EXPERIMENTAL DETAILS

The experiments were performed using a 90 kN, closed-loop, servo-hydraulic, test system fitted with an environmental chamber. The isothermal experiments were performed in vacuum, while the thermomechanical experiments were performed in flowing argon. A high temperature axial extensometer was used for strain measurement and control. Specimens were heated by a radio frequency induction generator. A chromel-alumel thermocouple was used for temperature measurement and control. The temperature profile along the gage length of a specimen was checked using three thermocouples, and less than a 10 °C variation was measured. A 16-bit computer was used to generate the strain and temperature waveforms, and to acquire the data.

Both the isothermal and thermomechanical experiments were performed in strain control at a constant mechanical strain rate. Prior to beginning the thermomechanical experiments, the temperature of the specimen was cycled between the desired limits, keeping the specimen at zero load. The temperature versus thermal-expansion strain data were stored and subsequently added to the desired mechanical strain waveform in order to obtain the control waveform. These thermal expansion strains were subtracted from the recorded total (thermal plus mechanical) strains in order to obtain the desired stress versus mechanical-strain hysteresis loops.

The material studied was polycrystalline OFHC copper supplied in the form of 19 mm round bars. Machined specimens were 120 mm in length, and had a 19 mm long uniform gage section. The diameter of the gage section was 9.5 mm. Each specimen was annealed at 538 °C for 1 hr in vacuum prior to testing.

DISCUSSION

There is a need for relatively simple viscoplastic models with the capability of providing accurate input to life assessing schemes. In high-temperature structural applications, three-dimensional stress states associated with nonisothermal and nonproportional loading histories are the norm, not the exception. The viscoplastic model presented herein was developed with this need and application in mind. To retain simplicity, it was essential to model only the first-order effects associated with the inelastic deformation of metals, such as isotropic and kinematic hardening. A second-invariant formulation for the flow equation was adopted, and as such, the higher order effect of distorting flow surfaces was neglected. Both the back stress and the drag stress evolve in a competitive process between strain-hardening and recovery. In particular, the back stress was considered to recover by a dynamic or strain-induced mechanism, while the drag stress was considered to recover by a static or thermally-induced mechanism. The static recovery of back stress and the dynamic recovery of drag stress were considered as higher-order effects, and have therefore been neglected. A significant simplification is achieved in the mathematical structure of the constitutive equations by not coupling static and dynamic recovery terms within either evolutionary equation. In this regard, the model is most unique. Each term and each material constant in the model has an interpretation that is physically meaningful. The phenomenological approach used to derive the material functions of this model is akin to the approach used by Miller (ref. 7) in his model development; however, our focus has been towards the simplified, whereas his focus is towards the detailed. In addition, our Zener-Hollomon parameter is similar to the one used by Miller (a hyperbolic sine raised to a power), but ours is more efficient in numerical integration. The end result is a relatively simple viscoplastic model with reasonable potential to achieve its objective. This model has recently been implemented into a finite-element code, where it is being used to perform structural analyses.

Thermomechanical experiments were performed for the purpose of assessing the model's capability under uniaxial conditions. A comparison between experiment and theory is presented in figure 4 for an in-phase test. Here the temperature range was from 200 to 500 °C, and the controlling mechanical strain rate was 1.5×10^{-5}/s. The model does a good job in predicting at the hot end of the cycle, but it over predicts at the cold end of the cycle. Problems in accurately predicting the cold end response of thermomechanical hysteresis loops seems to be a common flaw of viscoplastic models (ref. 16). Why this model exhibits an excessive amount of hardening at the cold end of the cycle is currently unknown. This is a disturbing result, since stress amplitude and mean stress are often important ingredients in life assessing schemes. Nevertheless, it is encouraging to note that the model predictions are more accurate than the often used rule-of-thumb, where stress amplitude and mean stress are determined from saturated isothermal hysteresis loops associated with the mechanical strain range and temperature extremes of the thermomechanical cycle.

The jagged nature of the experimental data is the result of strain avalanches (cf. Yan and Laird (ref. 17)). The digitally-stored data of figure 4 were acquired at too slow a rate to capture the details of the response. Figure 5 is an in-phase thermomechanical response curve for four consecutive cycles, which more clearly shows the substructure of the hysteresis loops associated with strain avalanches. Here the temperature range was from 316 to 427 °C, and the controlling mechanical strain rate was 2.5×10^{-5}/s. Yan and Laird observed this phenomena after cycling polycrystalline copper at room temperature to half life, while in the present work, strain avalanches were observed to begin at the onset of cycling in all thermomechanical experiments. The strain avalanches are not random, as evidenced by the coincidence of the four hysteresis loops. The spacing between the strain avalanches and the magnitude of the strain avalanches are related. The longer the time interval between two successive avalanches the larger the following avalanche.

REFERENCES

1. Freed, A.D.: Structure of a Viscoplastic Theory. NASA TM-100794, 1988.

2. Prager, W.: Recent Developments in the Mathematical Theory of Plasticity. J. Appl. Phys., vol. 20, no. 3, Mar. 1949, pp. 235-241.

3. Zener, C.; and Hollomon, J.H.: Plastic Flow and Rupture of Metals. Trans. Am. Soc. Metals, vol. 33, 1944, pp. 163-215.

4. Krieg, R.D.: A Practical Two Surface Plasticity Theory. J. Appl. Mech., vol 42, no. 3, Sept. 1975, pp. 641-646.

5. Mitra, S.K.; and McLean, D.: Work Hardening and Recovery in Creep. Proc. R. Soc. London Ser. A, vol. 295, no. 1442, Dec. 6, 1966, pp. 288-299.

6. Onat, E.T.; and Leckie, F.A.: Representation of Mechanical Behavior in the Presence of Changing Internal Structure. To appear in J. Appl. Mech., 1988.

7. Miller, A.K.: A Unified Phenomenological Model for the Monotonic, Cyclic, and Creep Deformation of Strongly Work-Hardening Materials. Ph.D. Thesis, Stanford University, 1975, pp. 36-41.

8. Ashby, M.F.: A First Report on Deformation-Mechanism Maps. Acta Met., vol. 20,
no. 7, July 1972, pp. 887-897.

9. Dorn, J.E.: Some Fundamental Experiments on High Temperature Creep. J. Mech. Phys. Solids, vol. 3, no. 2, Jan. 1955, pp. 85-116.

10. Odqvist, F.K.G.: Mathematical Theory of Creep and Creep Rupture. 2nd ed., Clarendon Press, Oxford, London, 1974, pp. 20-35.

11. Pahutova, M.; Cadek, J.; and Rys, P.: High Temperature Creep in Copper. Philos. Mag., vol 23, no. 183, Mar. 1971, pp. 509-517.

12. Barrett, C.R.; and Sherby, O.D.: Steady-State Creep Characteristics of Polycrystalline Copper in the Temperature Range 400 ° to 950 °C. AIME Trans., vol. 230, no. 6, Oct. 1964, pp. 1322-1327.

13. Feltham, P.; and Meakin, J.D.: Creep in Face-Centered Cubic Metals with Special Reference to Copper. Acta. Met., vol 7, no. 9, Sept. 1959, pp. 614-627.

14. Jenkins, W.D.; and Digges, T.G.: Creep of Annealed and Cold-Drawn High-Purity Copper. J. Res. NBS, vol. 47, no. 4, Oct. 1951, pp. 272-287.

15. Walker, K.P.; and Jordan, E.H.: Constitutive Modelling of Single Crystal and Directionally Solidified Superalloys. Turbine Engine Hot Section Technology 1987, NASA CP-2493, 1987, pp. 299-301.

16. Walker, K.P.: Personnal communication, 1988.

17. Yan, B.-D.; and Laird, C.: The Phenomenon of Strain Avalanches in Cyclic Deformation. Acta Met., vol. 33, no. 11, Nov. 1985, pp. 2023-2031.

TABLE I. - MATERIAL CONSTANTS FOR COPPER

Constant	Units	Values[a]
E	MPa	165,000 - 125T
α	$°C^{-1}$	$15x10^{-6} + 5x10^{-9}$ T
ν	-	0.34
A	s^{-1}	50,000,000
Do	MPa	1.5
h	MPa	500
H	MPa	5,000
L	MPa	25 exp(-T/300)
n	-	5
Q	J/mole	200,000
S	MPa	14.3
Tm	°K	1,356

[a]T is in degrees centigrade.

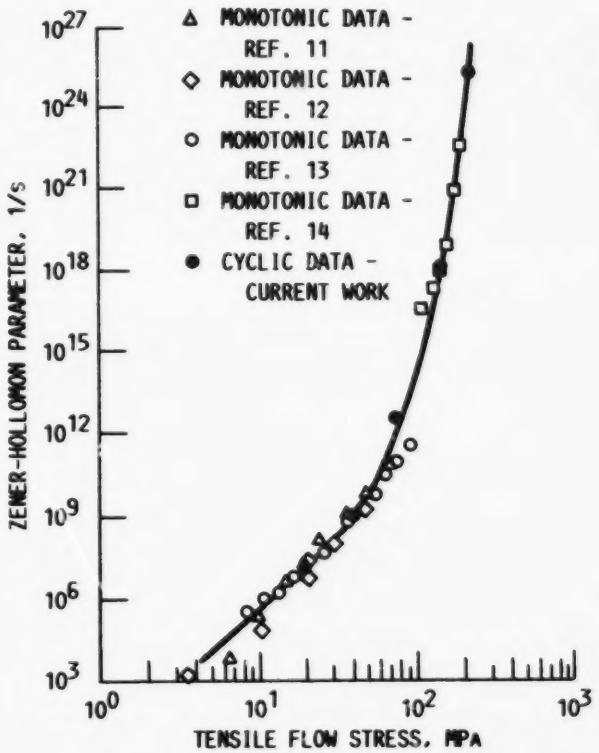

FIGURE 1. - STRESS DEPENDENCE OF THE ZENER-HOLLOMON PARAMETER FOR COPPER. THE CURVE IS THE FIT OF EQ. (7a) TO THESE DATA FOR THE MATERIAL CONSTANTS GIVEN IN TABLE I.

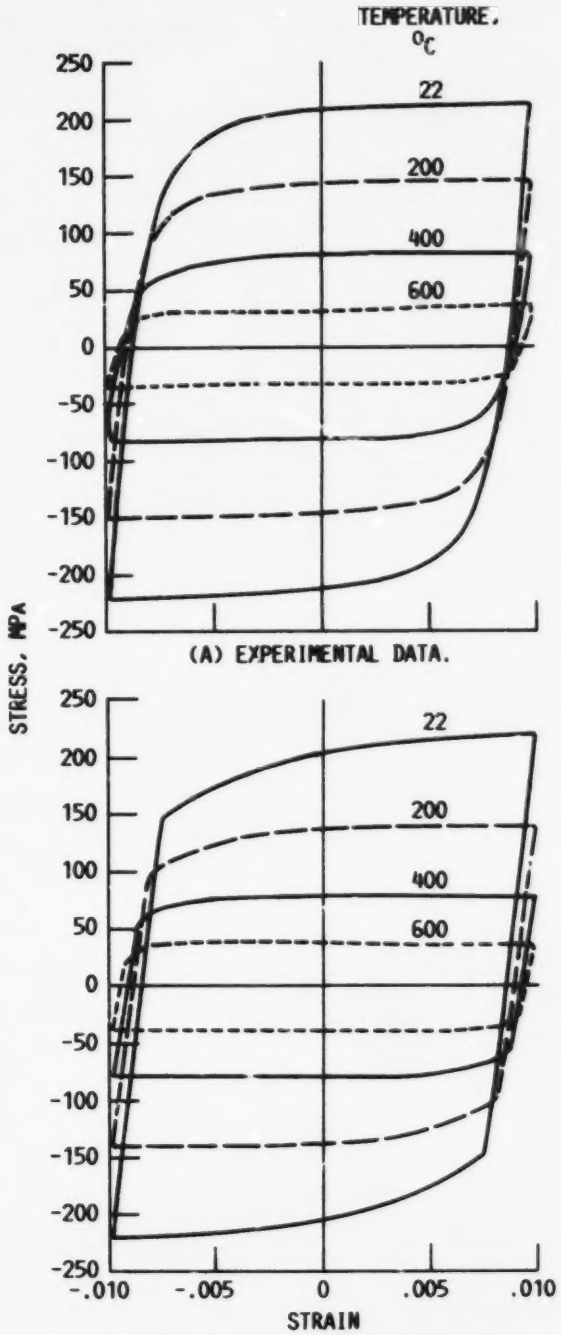

(A) EXPERIMENTAL DATA.

(B) THEORETICAL CORRELATIONS.

FIGURE 2. - SATURATED HYSTERESIS LOOPS FOR COPPER. $\dot{\epsilon}$ = 0.001/s.

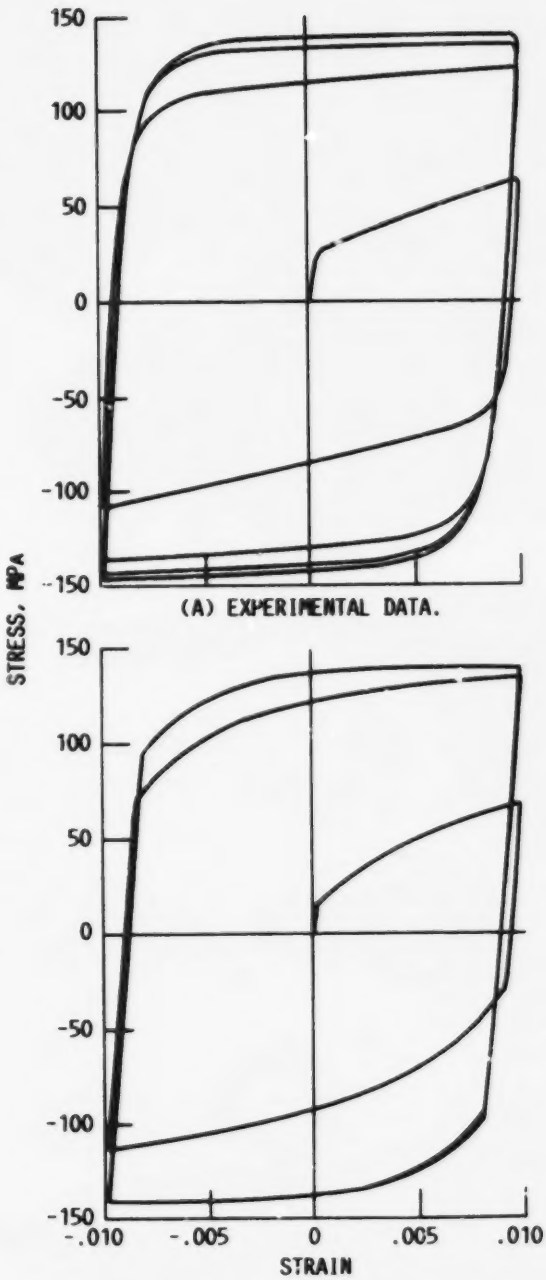

(A) EXPERIMENTAL DATA.

(B) THEORETICAL PREDICTION.

FIGURE 3. - STRESS-STRAIN RESPONSE OF COPPER. T = 200 °C; $\dot{\epsilon}$ = 0.001/s.

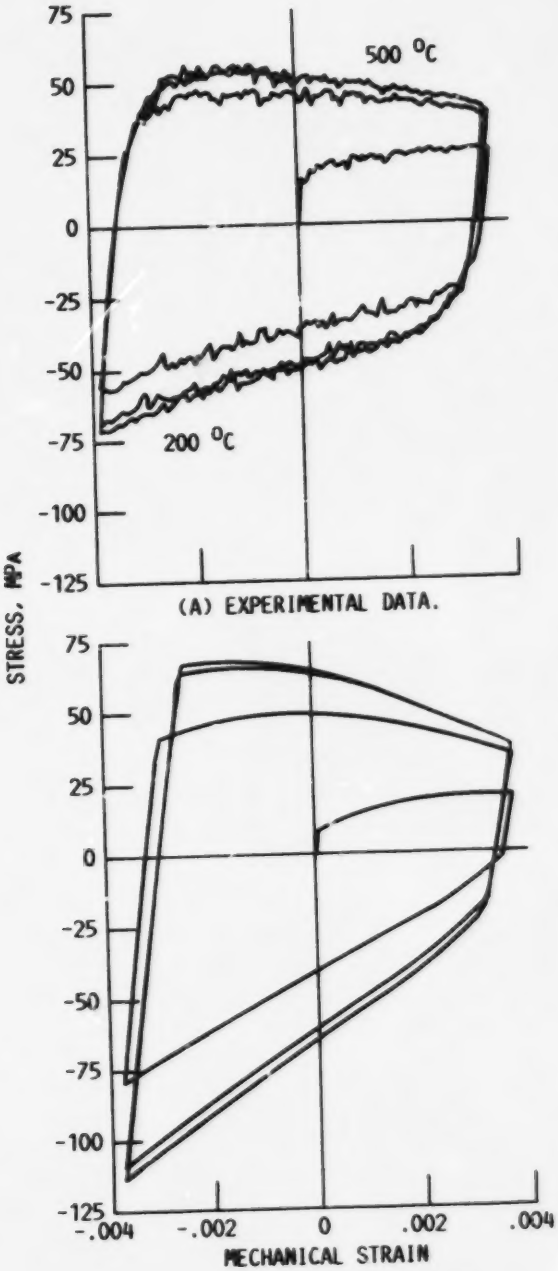

FIGURE 4. - IN-PHASE THERMOMECHANICAL HYSTERESIS LOOPS FOR COPPER. $\dot{\varepsilon} = 1.5 \times 10^{-5} + \alpha \dot{T}$ /s.

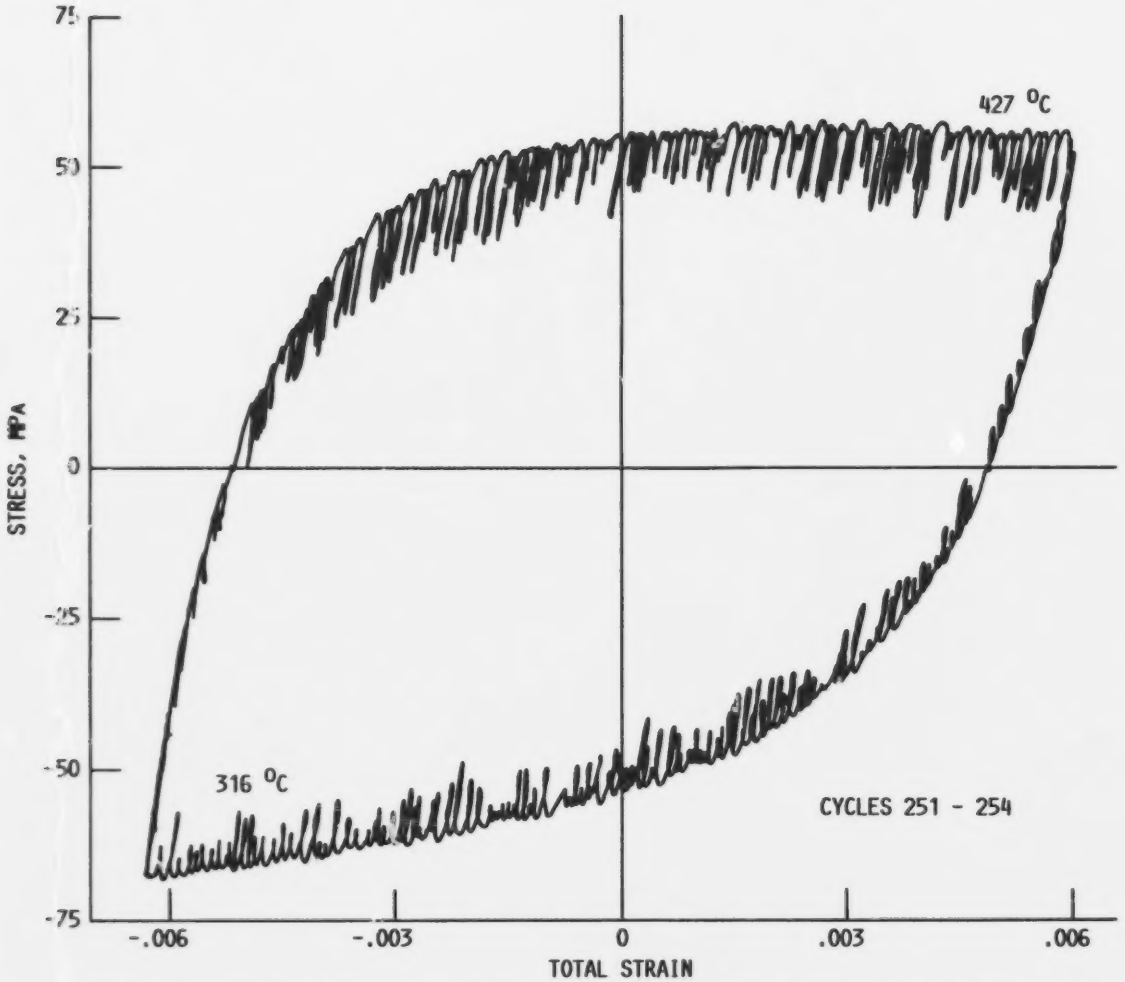

FIGURE 5. - IN-PHASE THERMOMECHANICAL HYSTERESIS LOOP FOR COPPER. $\dot{\varepsilon} = 2.5 \times 10^{-5} + \alpha \dot{T}$ /s.

NASA
National Aeronautics and Space Administration

Report Documentation Page

1. Report No.	2. Government Accession No.	3. Recipient's Catalog No.
NASA TM-100831		

4. Title and Subtitle

A Viscoplastic Theory Applied to Copper

5. Report Date

6. Performing Organization Code

7. Author(s)

Alan D. Freed and Michael J. Verrilli

8. Performing Organization Report No.

E-4020

10. Work Unit No.

505-63-1B

9. Performing Organization Name and Address

National Aeronautics and Space Administration
Lewis Research Center
Cleveland, Ohio 44135-3191

11. Contract or Grant No.

13. Type of Report and Period Covered

Technical Memorandum

12. Sponsoring Agency Name and Address

National Aeronautics and Space Administration
Washington, D.C. 20546-0001

14. Sponsoring Agency Code

15. Supplementary Notes

Prepared for the International Seminar on "The Inelastic Behavior of Solids Models and Utilization," sponsored by MECAMAT, Besançon, France, August 30 - September 1, 1988.

16. Abstract

A phenomenologically based viscoplastic model is derived for copper. The model is thermodynamically constrained by the condition of material dissipativity. Two internal state variables are considered. The back stress accounts for strain-induced anisotropy, or kinematic hardening. The drag stress accounts for isotropic hardening. Static and dynamic recovery terms are not coupled in either evolutionary equation. The evolution of drag stress depends on static recovery, while the evolution of back stress depends on dynamic recovery. The material constants are determined from isothermal data. Model predictions are compared with experimental data for thermomechanical test conditions. They are in good agreement at the hot end of the loading cycle, but the model over predicts the stress response at the cold end of the cycle.

17. Key Words (Suggested by Author(s))	18. Distribution Statement
Viscoplasticity; Creep; Thermodynamics; Copper; Stress-strain; Thermomechanical cycling	Unclassified - Unlimited Subject Category 39

19. Security Classif. (of this report)	20. Security Classif. (of this page)	21. No of pages	22. Price*
Unclassified	Unclassified	14	A02

NASA FORM 1626 OCT 86

*For sale by the National Technical Information Service, Springfield, Virginia 22161